

Comparative Investigation of the Adhesion of Ce Conversion Layers and Silane Layers to a AA 2024-T3 Substrate Through Mechanical and Electrochemical Tests

Luis Enrique Morales Palomino^a, Zoltán Pászti^b, Idalina Vieira Aoki^a, Hercílio Gomes de Melo^{a*}

^aEscola Politécnica da USP, Departamento de Engenharia Química,
Av. Prof. Luciano Gualberto, Trav. 3, n. 380,
Cidade Universitária, 05508-900 São Paulo - SP, Brazil

^bInstitute of Surface Chemistry and Catalysis, Chemical Research Center,
Hungarian Academy of Sciences, 59-67 Puztaszeri út, Budapest, Hungary, H-1025

Received: March 22, 2007; Revised: November 8, 2007

Cerium conversion layers and silane films are among the potential substitutes for the carcinogenic chromate conversion layers used to protect high-strength Al alloys. In the present work the adhesion of a cerium conversion layer and of a silane film to an aluminium alloy (AA) 2024-T3 substrate was investigated using mechanical and electrochemical tests. Scanning electron microscopy (SEM)- X ray energy dispersive spectroscopy (EDS), Fourier transform infrared spectroscopy (FT-IR) and X ray photoelectron spectroscopy (XPS) were used to characterize the layers prior and after the mechanical test consisting of ultrasonic rinse in deionized water during 30 minutes. Mechanically tested and untested layers were also submitted to electrochemical impedance spectroscopy (EIS) and anodic polarization measurements in 0.1 M NaCl solution. The results of the characterization tests have pointed to a stronger adhesion of the Ce layer to the substrate in comparison with the silane film, which was confirmed by the electrochemical tests. The adhesion between the silane film and the Ce conversion layer was also tested, to evaluate the possibility of using the system as a protective bi-layer in accordance with the new trends being developed to substitute chromate conversion layers.

Keywords: adhesion, AA 2024-T3, SEM-EDS, EIS, silane, cerium, FTIR, XPS

1. Introduction

AA 2024-T3 is largely used in aerospace applications. In this alloy, heterogeneous microstructure is intentionally developed to optimise mechanical properties. Unfortunately, the complex microstructure makes it susceptible to localized corrosion during service and complicates aqueous surface finishing processes¹⁻³.

It is widely known that 2xxx series alloys are among the most corrosion prone commercial materials in common use. The inhomogeneous distribution of Cu in these alloys microstructure has been shown to be a major cause for their low resistance to pitting and stress corrosion cracking. Specifically, the concentration of Cu in second-phase particles and the local depletion of Cu in certain microstructural regions establish local galvanic cell resulting in localized attack^{1,2}. Due to this fact, for commercial use, their corrosion resistance is improved by a complete coating system consisting of three individual layers: a conversion layer (pre-treatment), a primer and a topcoat⁴. In this system the substrate pre-treatment plays an important role on the corrosion resistance as it promotes adhesion with the primer and also imparts some corrosion protection⁵⁻⁷.

For many decades, chromate conversion coatings have been reported as the most efficient pre-treatment used as anti-corrosive inhibitors and adhesion promoters to the surface of AA employed in the aircraft industry^{4,8-12}. The use of chromates is, however, being restricted worldwide, as they are considered highly toxic and carcinogenic¹³⁻²⁰. Because current environmental legislation is moving towards total exclusion of Cr⁶⁺ of industrial processes, and due to tightening of regulatory pressures in order to reduce the hazardous waste of chromium, many attempts are being made to develop non-toxic alternative methods for corrosion protection of these materials. One of these non-toxic substitute treatments is based on the use of rare earth salts, in particular those of cerium^{13,17-21}.

Based initially on immersion treatments employing cerium salts as corrosion inhibitors, eg. CeCl₃, Ce ions have shown promising behavior as corrosion inhibitors for AA^{17,18}. Later, using conversion baths, Ce ions in solution were reported to form stable hydroxides/oxides films on the metal surface at locations of increased pH due to local cathodic activity^{13,19-21}. The deposition of Ce(OH)₃ and/or CeO₂ gives the films a distinctive yellow colour. Such chemical passivation process produces coatings that are more corrosion resistant than the naturally formed oxide film on the surface of AA^{19,20,22,23}, mainly due to polarization of the cathodic reaction. However, these films have been reported to have an inhomogeneous thickness²⁴. Recently the introduction of a pre-treatment step that provoked the deposition of a Cu-rich smut on the alloy surface seems to have overcome this latter drawback^{22,23}.

Recently pre-treatments based on the use of organofunctional silanes, in this work denominated simply silanes, have attracted the attention of researchers and industries^{25,26}. Silanes are known as good coupling agents and several tests have shown that they afford good corrosion protection to the base AA²⁵⁻³⁰. Silanes are hybrid organic-inorganic compounds with structure X₃Si(CH₂)_nY, where X represents a hydrolysable group such as methoxy or ethoxy, and Y is a functional group^{7,25,28} like an amine or a chain of sulphur atoms. When the silane is symmetrical about the functional group Y, e.g., if there are two Si bonded to three alkoxy (X₃) groups, these molecules are known as bis-functional silanes, having the structure X₃Si(CH₂)_nY(CH₂)_nSiX₃. On the other hand, when Y is just an alkyl chain we have a non-functional silane, which can be also mono or bis-functional. When a metallic substrate is immersed in a hydrolysed silane solution, the silanol groups bond to the metal surface through hydrogen bonds. Afterwards, upon heating up (curing) the silane-covered surface, con-

*e-mail: hgdemelo@usp.br

densation reactions occur and stable Si-O-Me and Si-O-Si covalent bonds are formed, giving rise to a dense polymeric network. It has been clearly demonstrated that the curing step results in a better corrosion protection of the metallic substrates^{7,16,29,31}, however protection degree also depends on such factors like the specific silane structure, the metal substrate²⁸, particularly insofar as it influences the nature of the interfacial bonding, as well as on processing details like silane concentration, hydrolysis time, and solution pH^{25,32}.

The aim of this study is to indirectly evaluate the bond strength of Ce conversion layers and silane layers to a AA 2024-T3 substrate. With this purpose samples coated with each one of the layers were characterized using SEM/EDS, FTIR and XPS prior and after being submitted to an adherence test consisting of immersion during 30 minutes in an ultrasonic bath^{5,6}. The use of such methodology in replacement of the traditionally used ASTM 3359-02³³ seemed to us more adequate as it equally test the coating adhesion all over the surface; however, for the sake of comparison, this test was also performed. Moreover the corrosion properties of samples submitted to the mechanical tests or not were assessed through EIS experiments and anodic polarization curves in 0.1 M NaCl solution.

As recent researches aiming to substitute chromate conversion layers are moving towards layers with more complex structure^{29,30,34-36}, in order to evaluate the affinity between Ce and silane layers, the same tests were performed with samples coated with a Ce-silane bi-layer.

2. Experimental Procedure

The AA 2024-T3 used in this work was supplied by a Brazilian industry (EMBRAER) as sheets with dimensions of (100 x 100 x 0.1) cm. This alloy has a high Cu content, typically between 3.8-4.9% (wt. (%))³⁷. The pre-treatment procedure used to prepare the samples for deposition of the Ce conversion layer has been described elsewhere as well as the conversion bath composition²³.

To obtain the silane coating the samples were prepared in the same manner as that used to produce the Ce conversion layer²³ with the difference that the Cu-rich smut left at the sample surface after immersion in the acetic acid solution was removed by vigorously washing.

The silane solution was prepared by adding 4% (w.w⁻¹) of BTSE (bis-1, 2-(triethoxysilyl) ethane) molecules to a 50%/50% (w.w⁻¹) ethanol/water solution, which, afterwards, had its pH adjusted to a value between 3.5 and 4 by the addition of acetic acid, and was left to hydrolyse during 30 minutes, according to the procedure described by Oliveira³⁸. It must be emphasized that the silane solution used in the present work was designed specifically to avoid the use of the carcinogenic methanol. To obtain the silane coatings, the pre-treated samples were immersed for 5 minutes in the hydrolysed solution at 25 °C. Next, the samples were left at rest for 2 minutes at room temperature and subsequently cured at 100 °C for 10 minutes which can be considered as a mild curing condition. The same procedure was adopted to obtain the top silane layer in the bi-layer coating, with the difference that the samples had been previously coated with the Ce conversion coating.

All the electrochemical tests were performed using a classical three electrodes cell with Ag/AgCl(sat.) and a platinum grid as reference and counter electrode, respectively, which were always positioned at the same place relatively to the working electrode (WE). Cell construction details can be found elsewhere^{22,23}. The experiments were performed in aerated conditions and at room temperature.

The set-up used to control the impedance experiments was composed of a Solartron 1260 frequency response analyzer (FRA) coupled to a Solartron 1287 electrochemical interface, the experiments were controlled by the software Corrware[®]. The diagrams were obtained

in the 10 kHz to 5 mHz frequency range, with an acquisition rate of 10 points per decade. The ac signal amplitude was 15 mV (rms). All the impedance experiments were performed at the OCP, which was recorded prior and after the measurement in order to verify the stationnarity.

Anodic potentiodynamic polarization curves were obtained at a 0.5 mV.sec⁻¹ scan rate using the same experimental set-up and electrochemical interface employed in the EIS experiments. The curve was initiated after the completion of the impedance measurements, i.e. after 72 hours of contact of the different samples with the test electrolyte, and finished when the total anodic current reached 1 mA.

SEM/EDS analyses were performed in all the coated samples and in the bare alloy. The equipment used was a Philips XL – 30 scanning microscope equipped with an EDS spectrometer. The acceleration voltage used to carry out the analyses was 20 keV, giving a penetration depth of approximately 1 µm. Semi-quantitative elemental analysis was executed using internal standards of the equipment. The mechanical adhesion test consisted in immersing the coated sample during 30 minutes in DI water containing ultrasonic bath.

The FT-IR technique is well known as a powerful tool in the field of polymer surface characterization. FT-IR measurements were conducted on a Bomem MB 100 spectrophotometer in the mid-IR range from 4000 to 400 cm⁻¹. All IR spectra were obtained at an incident angle of 75° normal to the surfaces of specimens, with a spectral resolution of 4 cm⁻¹.

XPS measurements were carried out using an electron spectrometer manufactured by OMICRON Nanotechnology GmbH (Germany). The photoelectrons were excited by AlK α (1486.6 eV) radiation. Spectra were recorded at normal emission in the Constant Analyser Energy mode.

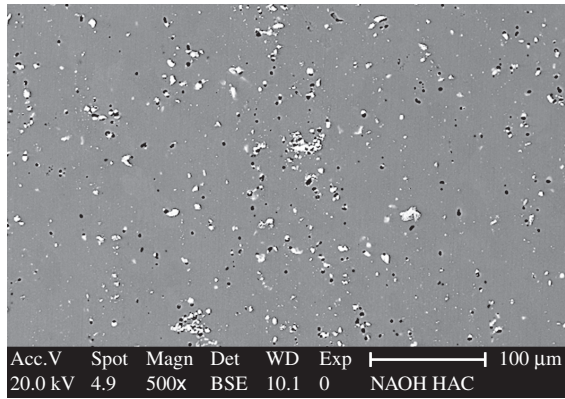
3. Results and Discussion

3.1. SEM characterization

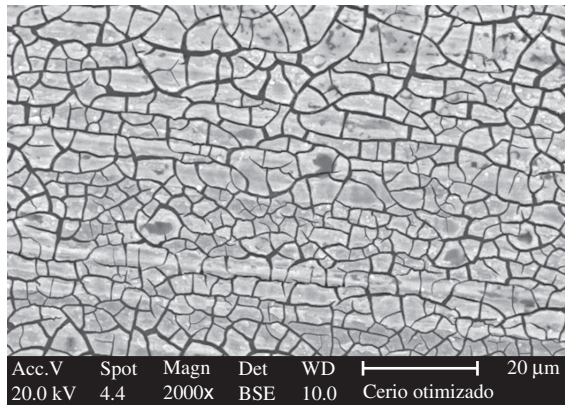
Figure 1 presents micrographs of the bare sample, Figure 1a, and of the AA 2024-T3 alloy coated with the different treatments: Ce conversion layer (Figure 1b), silane film (Figure 1c) and bi-layer Ce-silane (Figure 1d). These images have already been discussed elsewhere³⁹, however their main aspects will be highlighted. The bare sample presents coarse Al-Cu-Mg and Al-Cu-Fe-Mn intermetallics distributed on its whole surface, while, the Ce coated sample presents its usual dry-mud appearance. The presence of the silane layer on the sample surface is evident in Figure 1c, however it has been demonstrated that silanes does not adhere uniformly on Al surface^{5,6} the same was verified in the present work. In its turn, comparison of Figures 1b and 1d shows that the curing of the silane layer seems to introduce compressive stress (the cracks are longer and narrower) in the Ce conversion layer.

The micrographs of the coated samples after the mechanical test are presented in Figure 2. From the images is possible to observe that the coatings have been removed from the sample surface at different degrees. For the sample protected with the Ce-conversion layer (Figure 2a) large amounts of the coating has been removed. On the other hand, the detachment of the silane layer can be inferred due to the presence of the intermetallics (Figure 2b). For the last micrograph presented in this series (Figure 2c) it can be observed that the mechanical test removes only small amounts of the protective layer. This seems to indicate a synergetic action between the Ce and silane layers, in accordance with what had already been shown with the untested samples.

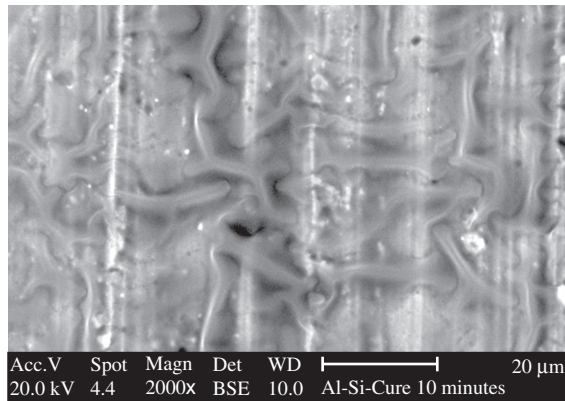
Figure 3a presents a comparison of the Si peaks intensities in EDS spectra for samples of AA 2024-T3 alloy coated with the different films before and after the adhesion tests. No difference was found in the analysis before the test, curves A and C, indicating that the silane



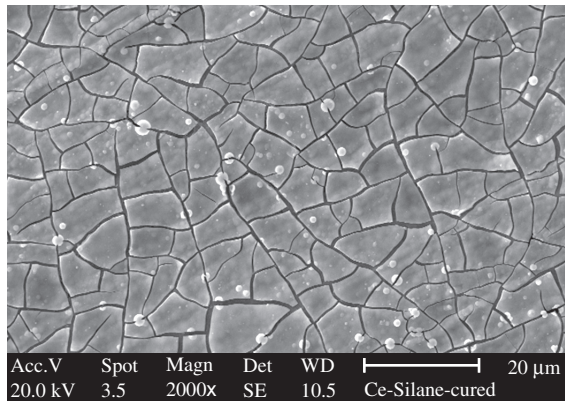
(a)



(b)

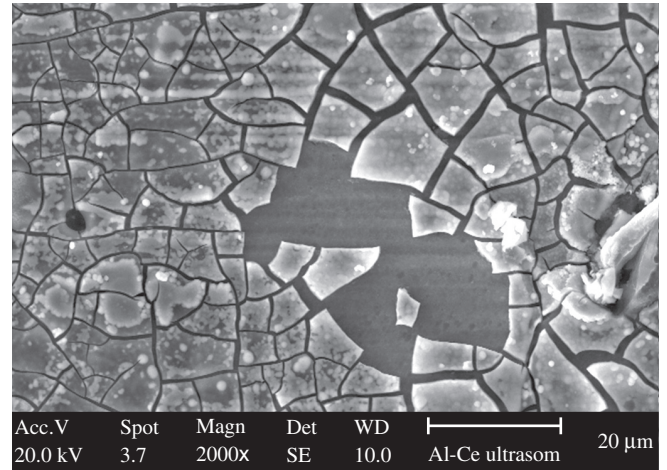


(c)

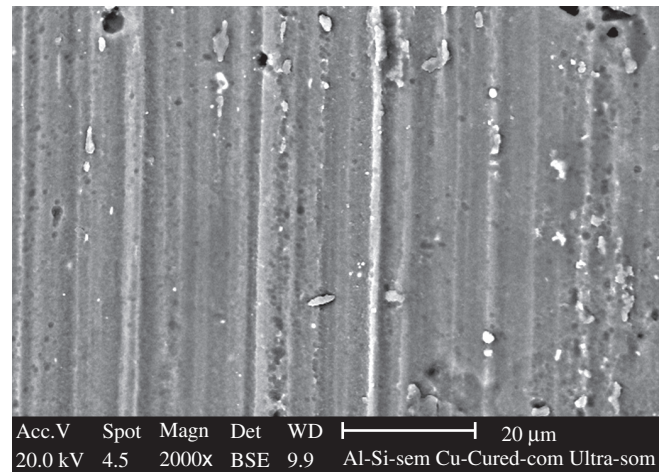


(d)

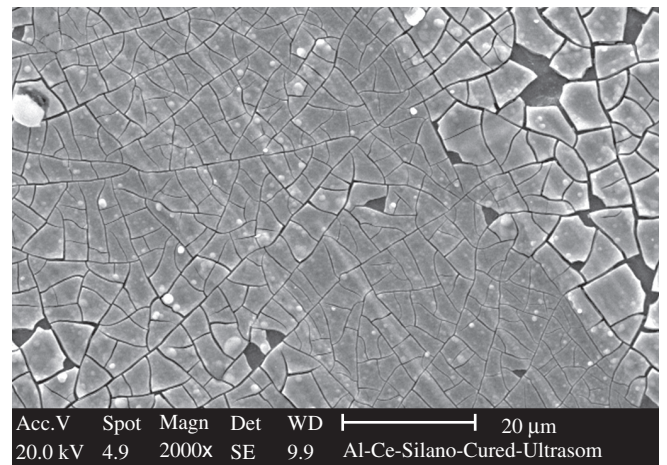
Figure 1. SEM micrographs of the AA 2024-T3 alloy. a) Bare (after the standard pre-treatment); b) Cerium coated; c) Silane coated; and d) Cerium-silane coated (cured).



(a)



(b)



(c)

Figure 2. SEM micrographs of the AA 2024-T3 alloy after the ultrasonic bath. a) Cerium coated; b) Silane coated; and c) Cerium-silane coated (cured).

molecules have equivalent affinity for both the bare alloy surface and for the Ce conversion layer. On the other hand, it is evident that the mechanical test removes almost all the silane molecules, curves B and D. However, the intensity of the Si peak in the Ce coated sample

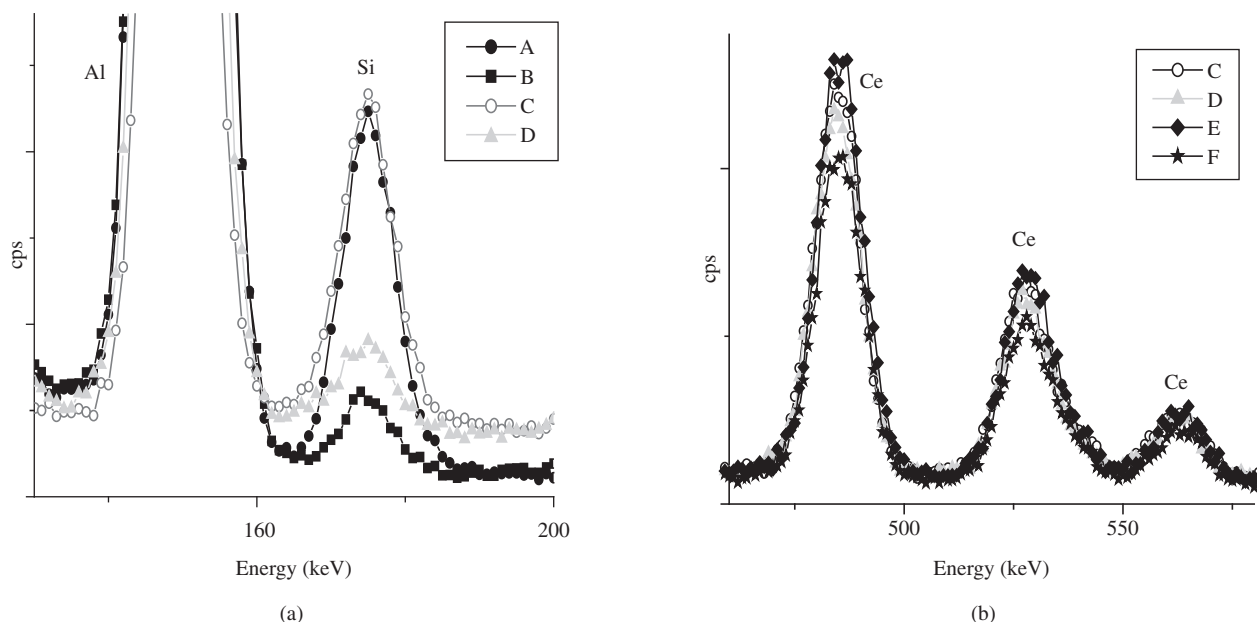


Figure 3. Si (A) and Ce (B) peaks intensity in EDS spectra of single- or bi-layer coated AA 2024-T3 samples prior and after the adhesion test: curve (A) Al-Si; curve (B) Al-Si – sonicated; curve (C) Al-Ce-Si; curve (D) Al-Ce-Si – sonicated; curve (E) Al-Ce; curve (F) Al-Ce – sonicated.

is stronger indicating a better interaction between the silane coating and the Ce conversion layer than with the Al substrate. On the other hand, the intensity of the peaks associated with Ce barely changes prior and after the mechanical tests indicating an excellent adhesion of the conversion layer to the metallic substrate.

3.2. FTIR characterization

Figure 4 shows the FTIR spectra of the BTSE silane film on samples submitted to the different treatments. The assignments of the characteristic absorption bands are given in Table 1^{7,31,40}. The bands in the SiOSi region, between 1000 to 1250 cm^{-1} , are clearly more intense in the bi-layer coated samples. According to the literature⁴⁰ the band at 1030 cm^{-1} is indicative of the formation of a long siloxane chain. The higher absorption intensity of this band for the Ce-silane coated sample suggests longer siloxane chains for this particular sample. On the other hand, the absorption intensities of the bands corresponding to silanol (SiOH) at, 3363, 3243 and 870 cm^{-1} are nearly the same for all the samples, indicating the existence of practically the same amount of non condensed silanol groups in all the samples. Finally, the bands belonging to the C-H stretching (CH_2 and CH_3) group: at 2972, 2924, and 2848 cm^{-1} are also more intense in the Ce-silane coated sample indicating a higher organization degree of the chains. Comparing the spectra obtained for the sonicated samples, (B) and (D), all the adsorption bands are more intense for the Ce-silane coated sample confirming the stronger adhesion of the silane layer to the Ce conversion coating, as already indicated in the EDS results.

3.3. XPS results

Survey XPS spectra taken for the silane coated AA samples with or without the Ce conversion layer confirmed the presence of C, Si, O, Al, Cu, Mg and – when appropriate – Ce. The amount of other contaminants was typically below the detection limit.

Figure 5 shows the Si and Al XPS spectra of the silane coated samples with or without the Ce conversion layer after curing, electrochemical and mechanical testing. All spectra were collected after small amount of ion bombardment, which does not seriously affect

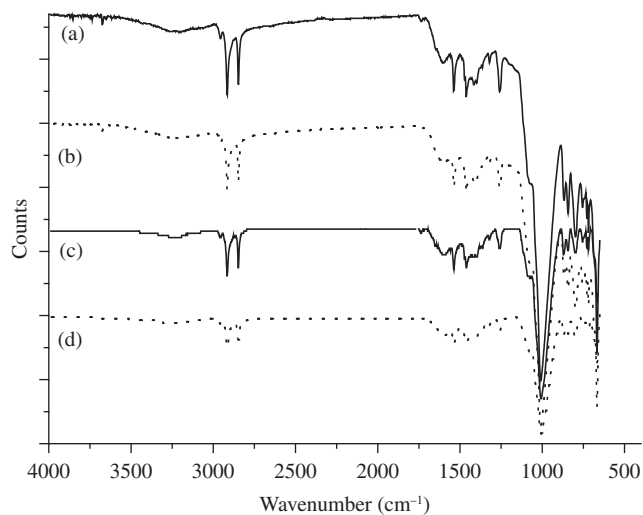


Figure 4. FT-IR spectra of the AA 2024-T3 sample with different treatments: a) Al-Ce-Si; b) Al-Ce-Si – sonicated; c) Al-Si; and d) Al-Si – sonicated.

Table 1. Absorption region and bond type found in silane films.

Wavelength (cm^{-1})	Bond type
700-800	C-H ($\text{Si-CH}_2\text{-CH}_2\text{-Si}$) stretching vibrations
850-900	Si-O (Si-OH) stretching vibrations
900-960	Si-O- C_2H_5 vibrations
1000-1250	Si-O (from Si-O-Si bonds) vibrations
1300-1400	CH_2 and CH_3 bending vibrations
1700-1750	C = O (acetic acid) stretching vibrations
2900-3000	C-H (CH_2 and CH_3) stretching vibrations
3200-3700	OH (from Si-OH group) stretching vibrations

the layer structure, but more or less removes the adventitious hydrocarbon contamination. The analysis of the figure shows that, in all cases, there is a measurable Al signal, most noticeable around 75 eV binding energy. This indicates that the coverage of the substrates by the different layers is never perfect. While the intensity of this signal is relatively weak for the cured (non-tested) and mechanically tested samples, the electrochemical test always significantly reduces the coverage, as indicated by the stronger intensity of the peak. Assuming that the silane layer thickness is much larger than

the information depth of the XPS and the Ce conversion layer is completely covered by the silane, the coverage of the substrate by the silane layer was calculated to be around 95-99% in the cases of the cured and mechanically treated samples, while for the electrochemical tested ones the values were around 75-80%.

3.4. EIS results

Figure 6 shows the Nyquist plots for AA 2024-T3 samples coated according to the different procedures presented in Figures 1 and 2. All

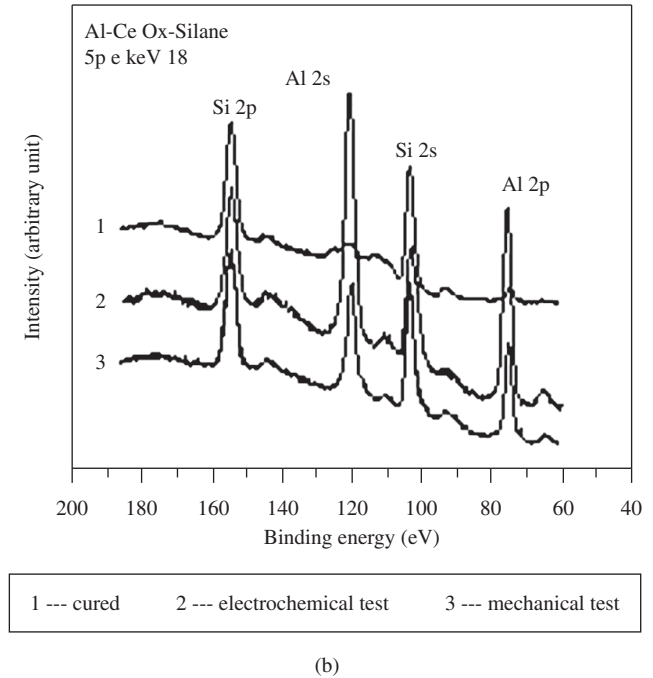
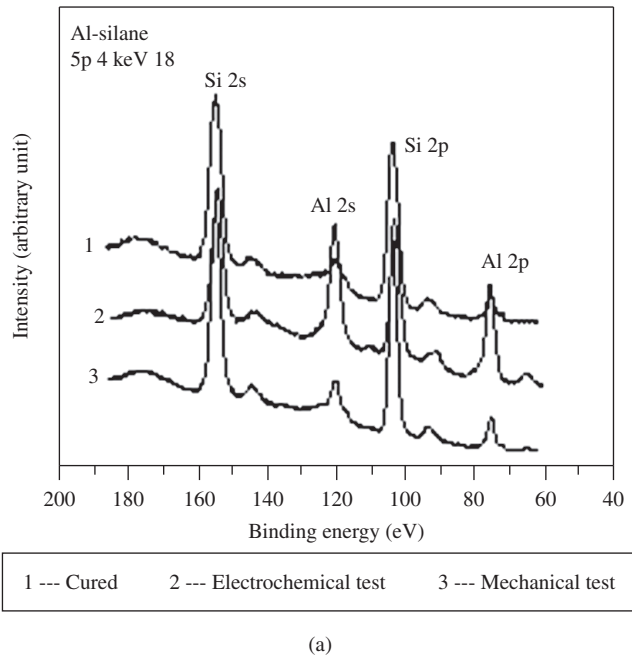


Figure 5. XPS analysis showing Al 2s and Si 2p signals from an AA 2024-T3 coated with Al-Si a), Al-Ce-Si b), before and after mechanical and electrochemical test.

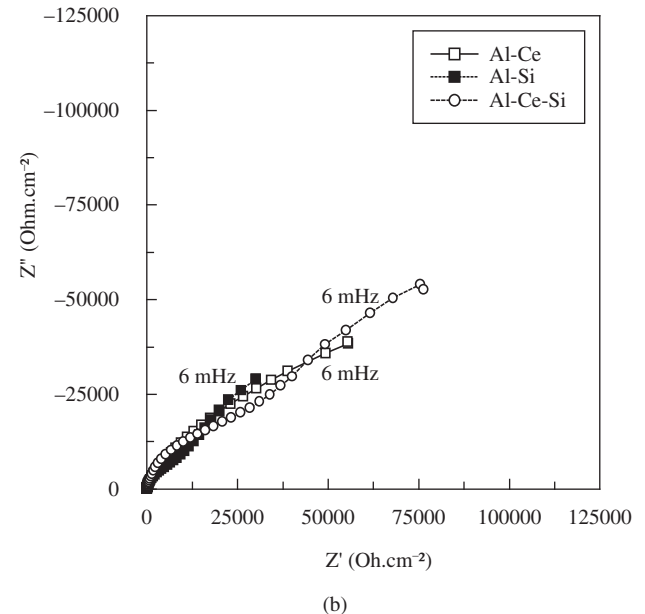
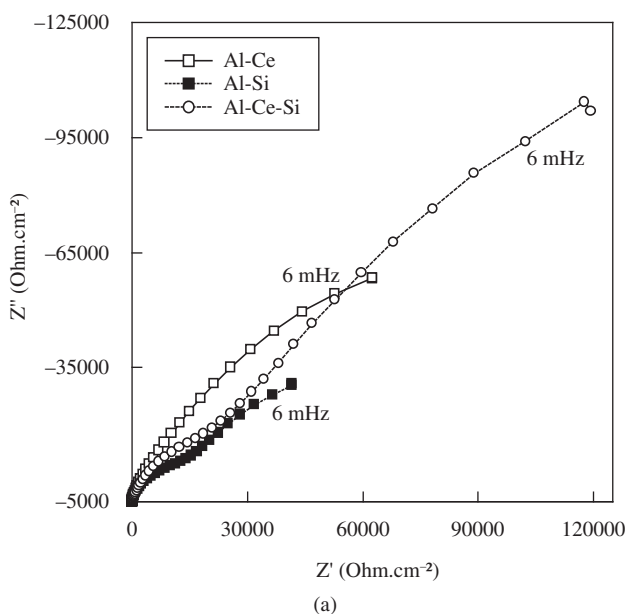


Figure 6. Impedance response in 0.1 M NaCl solution for AA 2024-T3 alloy with different treatments, a) before b) after ultrasonic bath. Immersion time 72 hours.

the impedance diagrams were obtained after 72 hours of immersion in the 0.1 M NaCl test solution. The results, before (A) and after (B) the ultrasonic bath test, show that the samples coated with the Ce-silane bi-layer present the best performance in the corrosion test.

Table 2 presents the values of the real impedance at 6 mHz (low frequency limit) extracted from the data presented in Figure 6. The values clearly shows a synergetic effect between the Ce conversion layer and the silane coating, once the low frequency impedance value is higher than the sum of the individual contributions. Moreover, the results also evidences the excellent adhesion of the Ce-conversion layer to the Al substrate, since, proportionally, the decrease in the real impedance value after the mechanical test was lower for this particular sample.

3.5. Anodic polarization behavior

The anodic polarization curves for the different samples, without and with the mechanical test, after 72 hours of immersion in the test electrolyte are presented in Figure 7a and b, respectively. The curves were obtained immediately after the completion of the impedance tests depicted in Figure 6. Comparing the response of samples with the same coating, a clear displacement of the currents to higher values was observed after the sonication test; however, the sample coated only with the silane layer suffered the stronger modification as the passive region almost disappeared after the mechanical test. Once more the bi-layer (Ce-silane) coated sample exhibited the best behavior.

3.6. Adhesion test according to ASTM D 3359-02³³

To confirm the good adhesion properties of the Ce conversion layer to the Al substrate, samples coated with only with the Ce

conversion layer and with the Ce-silane bi-layer were submitted to the tape pull-off test (ASTM D 3359-02)³³, the results are presented in Figure 8. Unfortunately, due to their transparent feature, the tests performed on samples coated only with the silane layer were inconclusive. The traditional test confirmed the good adhesion properties of the conversion layer to the base metal, as no detachment of the layer was verified after the test.

4. Conclusions

In this work a comparative investigation of the adhesion of Ce conversion layers and silane layers to a AA 2024-T3 substrate through mechanical and electrochemical tests was performed. The results of the analytical techniques (FT-IR, EDS and XPS) evidenced that silane molecules have equivalent affinity to the Al substrate and to the Ce conversion layer. Moreover, SEM-EDS observations in samples previously submitted to ultrasonic bath testing put in evidence an excellent adhesion of the Ce layer to the surface of the alloy. This was improved in the sample coated with the bi-layer Ce-silane, evidencing a synergistic effect of the Ce conversion layer and the silane coating.

The performance analysis through EIS and anodic polarization curves indicated superiority of the bi-layer, before ultrasonic bath, in comparison with samples protected by only a monolayer of cerium or silane. Additionally, after the application of the mechanical test the impedance values were still higher than the samples coated with only a monolayer not submitted to any type of mechanical test, ratifying the observations of good adhesion properties of the bi-layer to the substrate.

In addition, the results of FT-IR showed a slightly increase of the formation of siloxane structures (Si-O-Si) for the sample with bi-layer (Ce-silane) before ultrasonic bath, which may play a critical role in the corrosion protection process, as evidenced in the results of the electrochemical tests.

Acknowledgments

The author Hercílio Gomes de Melo is thankful to FAPESP, São Paulo state (Brazil) research financing agency for the financial sup-

Table 2. Real impedance at 6 mHz for AA 2024-T3 coated according to the different procedures prior and after the sonication test. Immersion time 72 hours.

Treatment	Al-Ce	Al-Si	Al-Ce-Si
Before ultrasonic bath Ohm.cm ⁻² (6 mHz)	52746	36471	102310
After ultrasonic bath Ohm.cm ⁻² (6 mHz)	46265	25894	67892

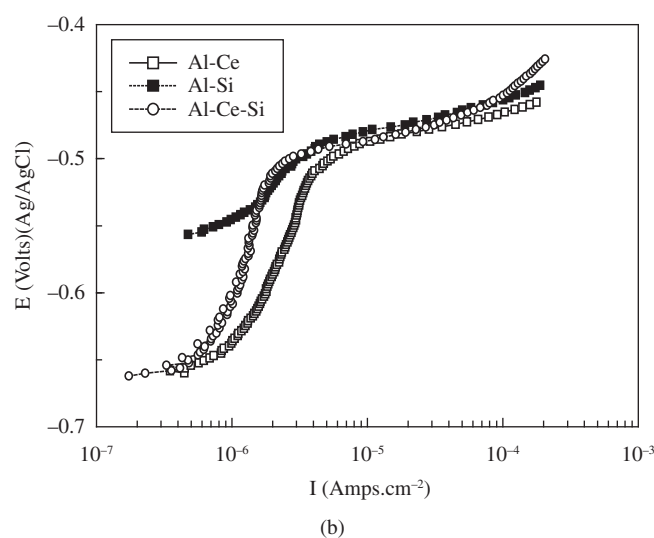
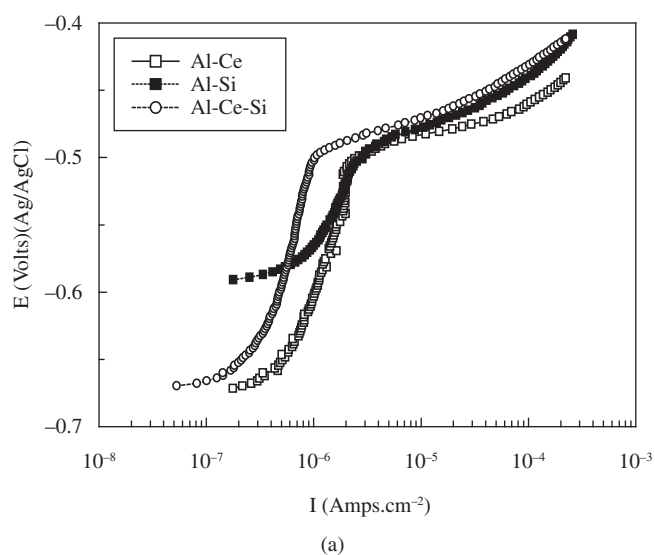
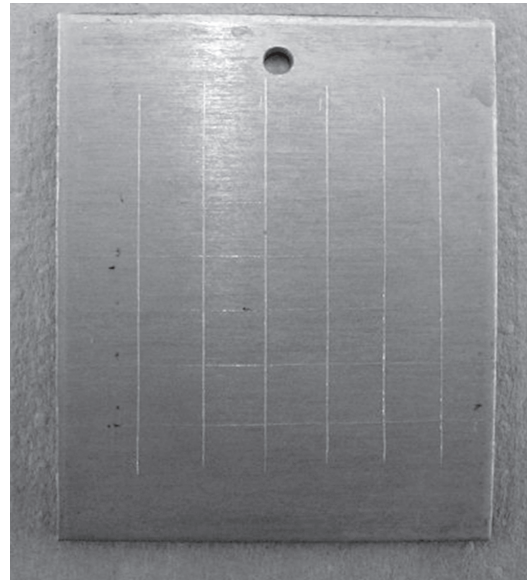


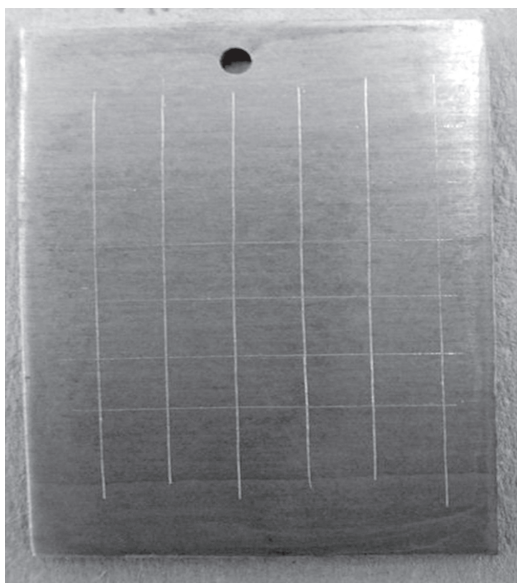
Figure 7. Anodic polarization curves in 0.1 M NaCl solution for AA 2024-T3 with different treatments. Curves obtained after the impedance experiments presented in Figure 6; a) non-sonicated; and b) sonicated samples.



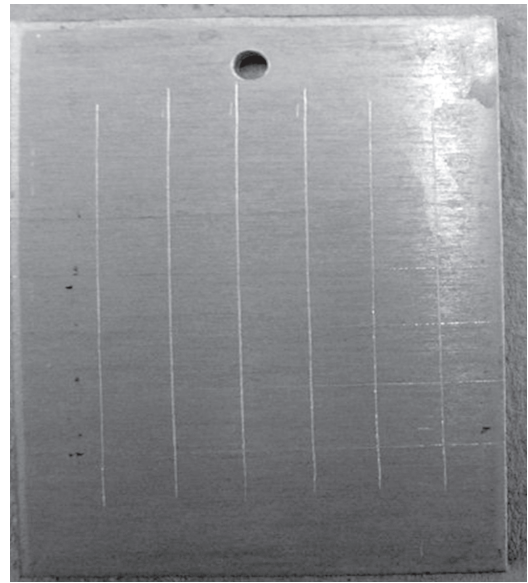
(a1)



(a2)



(b1)



(b2)

Figure 8. Sequence of the adhesion test on surface AA 2024-T3, with Ce-conversion layer (a1, b1) and bi-layer Ce-silane (a2, b2). Images obtained with digital camera.

port and Luis E.M. Palomino is thankful to CNPq, Brazilian research financing agency for the grant.

References

- Buchheit RG, Grant RP, Hlava PF, Mckenzie B, Zender GL. Local dissolution phenomena associated with S phase (Al_2CuMg) particles in aluminum alloy 2024-T3. *Journal of the Electrochemical Society*. 2002; 144(8):2621-2628.
- Guillaumin CH, Mankowski G. Localized corrosion of 2024 T351 aluminum alloy in chloride media. *Corrosion Science*. 1998; 41(3):421-438.
- Blanc C, Gastaud S, Mankowski G. Mechanistic Studies of the Corrosion of 2024 Aluminum Alloy in Nitrate Solutions. *Journal of the Electrochemical Society*. 2003; 150:B396-B404.
- Palanivel V, Huang Y, van Ooij WJ. Effects of addition of corrosion inhibitors to silane films on the performance of AA2024-T3 in a 0.5M NaCl solution. *Progress in Organic Coatings*. 2005; 53(2):153-168.
- Teo M, Kim J, Wong PC, Wong KC, Mitchell KAR. Pre-treatments applied to oxidized aluminum surfaces to modify the interfacial bonding with bis-1,2-(triethoxysilyl)ethane (BTSE): Part I. High-purity Al with native oxide. *Applied Surface Science*. 2005; 252(5):1293-1304.
- Teo M, Kim J, Wong PC, Wong KC, Mitchell KAR. Pre-treatments applied to oxidized aluminum surfaces to modify the interfacial bonding with bis-1,2-(triethoxysilyl)ethane (BTSE): Part II. Anodized 7075-T6 Al alloy. *Applied Surface Science*. 2005; 252(5):1305-1312.
- Franquet A, Pen CL, Terryn H, Vereecken J. Effect of bath concentration and curing time on the structure of non-functional thin organosilane layers on aluminium. *Electrochimica Acta*. 2003; 48(9):1245-1255.

8. Schneider M, Lohrengel MM, Rosenkranz C, Schreiber A, Kock E, Beneke M. *Proceedings of the 3rd International Symposium on Aluminium Surface Science and Technology*, Bonn, Germany 2003. p. 247.
9. Hughes AE, Taylor RJ, Hinton B. Chromate conversion coatings on 2024 Al alloy. *Surface and Interface Analysis*, 1997; 25(4):223-234.
10. Goeminne G, Terryn H, Vereecken J. EIS study of the influence of aluminium etching on the growth of chromium phosphate conversion layer. *Electrochimica Acta*, 1998; 43(12-13):1829-1838.
11. Campestrini P, Westing V, Wit JH. Influence of surface preparation on performance of chromate conversion coatings on Alclad 2024 aluminium alloy Part II: EIS investigation. *Electrochimica Acta*. 2001; 46(17):2631-2647.
12. Akiyama E, Markworth AJ, McCoy JK, Frankel GS, Xia L, McCreery RL. Storage and release of soluble hexavalent chromium from chromate conversion coating on Al alloys. *Journal of the Electrochemical Society*. 2003; 150(2):83-91.
13. Aldykewicz AJ, Davenport AJ, Isaacs HS. The investigation of cerium as a cathodic inhibitor for aluminum-copper alloys. *Journal of the Electrochemical Society*. 1995; 142:3342-3350.
14. Domingues L, Oliveira C, Fernandes J, Ferreira M, Fonseca I. Corrosion behaviour of environmentally friendly treatments for aluminium alloys. *Advanced Materials Forum I*. 2002; 230(2):392-395.
15. Lewington TA, Alexander MR, Thompson GE, McAlpine E. Characterisation of alkyl phosphonic acid monolayers self assembled on hydrated surface of aluminium. *Surface Engineering*. 2002; 18(3):228-232.
16. Subramanian V, Van Ooij WJ. Silane based metal pretreatments as alternatives to chromating: Shortlisted. *Surface Engineering*. 1999; 15(2):168-172.
17. Hinton BRW, Arnot DR, Ryan NE. The inhibition of aluminium alloy corrosion by cerous cations. *Metals Forum*. 1984; 7(4):211-217.
18. Hinton BRW, Arnot DR, Ryan NE. Cerium conversion coatings for the corrosion protection of aluminium. *Metals Forum*. 1986; 9(3):162-73.
19. Xingwen Y, Chunan C, Zhiming Y, Derui Z, Zhongda Y. Study of double layer rare earth metal conversion coating on aluminum alloy LY12. *Corrosion Science*. 2001; 43(7):1283-1294.
20. Xingwen Y, Chunan C, Zhiming Y, Derui Z, Zhongda Y. Corrosion behavior of rare earth metal (REM) conversion coatings on aluminum alloy LY12. *Materials Science and Engineering A*. 2003; 284(10):56-63.
21. Campestrini P, Terryn H, Hovestad A, Wit JHW. Formation of a cerium-based conversion coating on AA2024: relationship with the microstructure. *Surface and Coatings Technology*. 2004; 176(3):365-381.
22. Palomino LEM, de Castro JF, Aoki IV, de Melo HG. Microstructural and electrochemical characterization of environmentally friendly conversion layers on aluminium alloys. *Journal of the Brazilian Chemical Society*. 2003; 14(4):651-659.
23. Palomino LEM, Aoki IV, de Melo HG. Microstructural and electrochemical characterization of Ce conversion layers formed on Al alloy 2024-T3 covered with Cu-rich smut. *Electrochimica Acta*. 2006; 51(26):5943-5953.
24. Hughes AE, Taylor RJ, Hinton BRW, Wilson L. XPS and SEM characterization of hydrated cerium oxide conversion coatings. *Surface and Interface Analysis*. 1995; 23(7-8):540-550.
25. van Ooij, WJ. Child TF. Protecting metals with silanes coupling agents. *Chemtech*. 1998; 29(2):26-35.
26. Franquet A, De Laet J, Schram T, Terryn H, Subramanian V, van Ooij WJ, Vereecken. Determination of the thickness of thin silane films on aluminium surfaces by means of spectroscopic ellipsometry. *Thin Solid Films*. 2001; 384(1):37-45.
27. Cabral A, Duarte RG, Montemor MF, Zheludkevich ML, Ferreira MGS. Analytical characterisation and corrosion behaviour of bis-[triethoxysilylpropyl]tetrasulphide pre-treated AA2024-T3. *Corrosion Science*. 2005; 47(3):869-881.
28. Zhu, D, van Ooij WJ. Enhanced corrosion resistance of AA 2024-T3 and hot-dip galvanized steel using a mixture of bis- triethoxysilylpropyl] tetrasulfide and bis- trimethoxysilylpropyl]amine. *Electrochimica Acta*. 2004; 49(7):1113-1125.
29. van Ooij, WJ, Zhu D. Electrochemical impedance spectroscopy of bis-triethoxysilylpropyl]tetrasulfide on Al 2024-T3 substrates. *Corrosion*. 2001; 57(5):413-427.
30. Zhu D, van Ooij, WJ. Corrosion protection of AA 2024-T3 by bis-[3-(triethoxysilyl)propyl]tetrasulfide in sodium chloride solution.: Part 2: mechanism for corrosion protection. *Corrosion Science*. 2003; 45(10):2177-2197.
31. Franquet A, Terryn H, Vereecken J. IRSE study on effect of thermal curing on the chemistry and thickness of organosilane films coated on aluminium. *Applied Surface Science*. 2003; 211(1-4):259-269.
32. Susac D, Sun X, Mitchell KAR. Adsorption of BTSE and γ -APS organosilanes on different microstructural regions of 2024-T3 aluminum alloy. *Applied Surface Science*. 2003; 207(1-4):40-50.
33. American Society for Testing and Materials. *ASTM D 3359-02*. Standard test methods for measuring adhesion by tape test; 1987.
34. Kowayashi Y, Fujiwara Y. Corrosion protection of cerium conversion coating modified with a self-assembled layer of phosphoric acid mono-n-alkyl ester. *Electrochemical and Solid-State Letters*. 2006; 9(3):B15-B18.
35. Montemor MF, Cabral AM, Zheludkevich ML, Ferreira MGS. The corrosion resistance of hot dip galvanized steel pretreated with Bis-functional silanes modified with microsilica. *Surface and Coatings Technology*. 2006; 200(9):2875-2885.
36. Ferreira MGS, Duarte RG, Montemor MF, Simões AMP. Silanes and rare earth salts as chromate replacers for pre-treatments on galvanised steel. *Electrochimica Acta*. 2004; 49(17-18):2927-2935.
37. ALCOA. Alcoa Inc. Pittsburgh 2005 [cited 2006 Aug 20] Available from: www.alcoa.com/aerospace/en/product.
38. Oliveira, F. M. *Estudo da influência de organo-silanos na resistência à corrosão de aço-carbono por meio de técnicas eletroquímicas*. [PhD thesis]. São Paulo University: São Paulo; 2006.
39. Palomino LEM, Pacifico IA, Aoki IV, de Melo HG. *EIS investigation of the behaviour of double layer Cerium - Silane pre-treatment on Al 2024-T3 in 0.1M NaCl*. In: *The European Corrosion Congress; 2005. Proceedings. SPM/ EFC, Lisboa 2005*. p. 411.
40. Zhu, D. *Corrosion protection of metals by silane surface treatment*. [PhD thesis]. University of Cincinnati: Ohio; 2005.